

Tribol Lett (2009) 35:105–112  
DOI 10.1007/s11249-009-9437-3

ORIGINAL PAPER

# Temperature Effect on a HDD Slider's Flying Performance at Steady State

Nan Liu · David B. Bogy

Received: 30 December 2008 / Accepted: 17 March 2009 / Published online: 28 March 2009  
© The Author(s) 2009. This article is published with open access at [Springerlink.com](http://Springerlink.com)

**Abstract** The temperature inside modern hard disk drives (HDDs) can become as high as 100°C during operation. The effects of such high temperatures on the slider's flying attitude and the shear forces on the slider and the disk are investigated in this paper. General formulae for the shear forces are derived, and the generalized Reynolds equation is modified to take into account the temperature effect on the mean free path of air as well as the air viscosity. Numerical results are obtained for two different air bearing surface designs. It is shown that the temperature changes result in non-negligible changes in the slider's flying height and the shear forces. These changes could further induce changes in the deformation and instability of the lubricant layer and thereby affect the reliability of the HDDs.

**Keywords** Air bearings · HDD reliability · Temperature effect

## 1 Introduction

In modern hard disk drives (HDDs), the temperature inside the HDDs can rise to as high as 100°C. Since the temperature is related to the gas molecules' speed [1], the temperature increase affects the motion of the air molecules in the head-disk interface (HDI), which is the gap between the slider and the disk in the HDDs as shown in Fig. 1. Due to its dependence on the motion of the air molecules, the slider's flying performance is affected by the temperature

change as well. In this paper, we focus on two important issues of HDD slider's flying performance at steady state: the slider's flying attitude and the shear forces on the slider and the disk. The slider's flying attitude, including the slider's flying height, pitch and roll angles, is related to the capacity of the HDDs. According to Wallace's equation [2], the capacity of a HDD is inversely related to the slider's flying height at the read–write element, which is located at the trailing edge of the slider. Thus, a lower flying height and a more stable flying attitude of the slider are critical to the increase of the HDDs' capacity. The shear forces on the slider and the disk are related to the reliability of HDDs. As shown in Fig. 1, the magnetic disk, which is used to store the data, is actually covered by a thin layer of lubricant, which serves to reduce the possibility of the slider's contact onto the disk. The shear force on the lubricant has been shown to be the dominant factor determining the deformation and instability of the lubricant layer [3, 4]. This deformation and instability serve as a mechanism for the transfer of the lubricant from the disk to the slider [5], which increases the likelihood of the slider's impact on the disk and can result in wear of the disk as well as the loss of data stored on the disk.

Cha et al. [6] numerically solved the classical Reynolds equation for a slider with a minimum flying height around 60 nm, and they qualitatively argued that an increase in temperature induced increases in both the mean free path  $\lambda$  and the air viscosity  $\mu$ . The increases in  $\lambda$  and  $\mu$  led to opposite effects on the slider's flying height and finally resulted in a small change in the slider's flying height. Their experiments confirmed this qualitative argument and showed that the flying height only changed by 1 nm when the temperature increased by 20°C. Since the minimum flying height of the slider in the current HDDs is <10 nm and is being reduced to <5 nm, the classical Reynolds

N. Liu (✉) · D. B. Bogy  
Computer Mechanics Laboratory, Department of Mechanical Engineering, University of California, 5146 Etcheverry Hall, Berkeley, CA 94720, USA  
e-mail: [nanliu@me.berkeley.edu](mailto:nanliu@me.berkeley.edu)

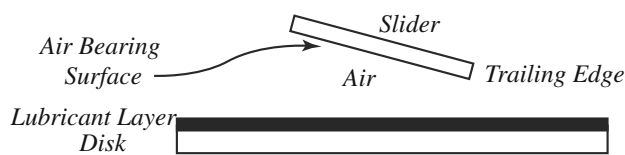


**Fig. 1** The HDI is composed of a slider, a disk, and the air gap in between. A layer of lubricant covers the disk and serves to reduce possible impact of the slider on the disk

equation is no longer applicable, and a change of 1 nm or so in the slider’s flying height, if it exists, is no longer a negligible change. Zhang et al. [7] also studied the temperature effect on the slider’s flying height when investigating the effect of humidity on the slider’s flying performance at different temperatures. They, however, did not provide any details on how they included the temperature effect into their simulations. Even less work has been done on the shear forces on the slider and the disk when compared to studies on the temperature effect on the slider’s flying attitude. In the current air bearing surface (ABS) design program, the hard sphere (HS) model for air molecules is used to study the temperature effect on the slider’s flying performance, and the analytical results based on the first-order slip theory are used to calculate the shear forces on the slider and the disk. Since the HS model can at most give qualitative results for the temperature dependence of air viscosity and the mean free path of air molecules, more refined models are needed. At the same time, the air gap thickness in the HDI is comparable or even less than the mean free path, and the first-order slip theory does not hold in the entire HDI. Thus, a study of the temperature effect on the slider’s flying performance and interface shear is needed.

In this paper, we modify the generalized Reynolds equation, which is derived from the Boltzmann equation, by using a variable soft sphere (VSS) model for the air molecules to include a temperature effect on the mean free path and air viscosity. The formulae for the shear forces are also derived and serve as a basis for the study on how temperature increase affects the shear forces on the slider and the disk. This paper is organized as follows. The formulae for the shear forces on the slider and the disk are derived in Sect. 2. In Sect. 3, we review and modify the generalized Reynolds equation. Numerical results are presented and discussed in Sect. 4. Finally, a summary and conclusion are given in Sect. 5.

## 2 Shear Forces on the Slider and the Disk

In current HDDs, the slider’s minimum flying height is around 10 nm, and the thickness of the air gap in the HDI,  $h$ , ranges from several nanometers to several micrometers. Since the mean free path of air is around 65 nm, the air in the

HDI is rarefied, and the Knudsen number in the HDI, defined as  $Kn = \lambda/h$ , changes from  $<0.1$  to  $>10$ . It is generally known that continuum theory, even supplemented with slip boundary conditions, applies only when the Knudsen number is  $<0.1$  [8]. Thus, continuum theory cannot describe air flow in current HDIs, where kinetic theory is needed.

Flow of a rarefied gas is described by the Boltzmann equation, which, for a steady problem with no external forces, such as the present one, reduces to [1]

$$\xi_i \frac{\partial f}{\partial x_i} = J(f, f), \tag{1}$$

where  $f$  is the velocity distribution function of the gas molecules,  $x_i$  are Cartesian coordinates, and  $\xi_i$  are the molecular velocity with  $i$  ranging over 1, 2, 3, and the summation convention is used.  $J(f, f)$  is a complicated integral whose exact form is not of concern here.

In view of the complexity of the Boltzmann equation, Eq. 1, Bhatnagar, Gross and Krook [9] proposed a model equation, namely the BGK–Boltzmann equation, by using  $v(f_e - f)$  to replace the right hand side of Eq. 1. Here  $v$  is a collision frequency that is related to the mean free path of the gas, and  $f_e$  is a local Maxwellian which has the same form as the Maxwellian distribution function but with its parameters determined by  $f$ . Despite its simple form, the BGK–Boltzmann equation is a nonlinear equation because of the appearance of  $f$  in  $f_e$ . When the velocity of the flow is much less than the average thermal velocity of the gas, the BGK–Boltzmann equation can be linearized by substituting  $\phi = ff_0 - 1$  into the BGK–Boltzmann equation, i.e. Eq. 1 with its right hand side replaced by  $v(f_e - f)$ , and retaining only linear terms. Here  $f_0$  is the Maxwellian distribution at the ambient state:

$$f_0 = \frac{\rho_0}{(2\pi RT_0)^{3/2}} \exp\left(-\frac{\xi_i \xi_i}{2RT_0}\right), \tag{2}$$

where  $\rho_0$ ,  $T_0$  are the ambient density and the ambient temperature, respectively, and  $R$  is the specific gas constant. The linearized BGK–Boltzmann equation for a steady flow of an isothermal gas is

$$\xi_i \frac{\partial \phi}{\partial x_i} = v \left( -\phi - 1 + \frac{\rho}{\rho_0} + \frac{\xi_i v_i}{RT_0} \right). \tag{3}$$

The corresponding boundary condition accompanying Eq. 3, after it is linearized, is [10]

$$\begin{aligned} \phi(x_i, \xi_i) = & (1 - \alpha)\phi(x_i, \xi_i - 2\xi_j n_j n_i) \\ & - \alpha \frac{2\sqrt{\pi}}{(2RT_0)^2} \int_{\xi_k n_k < 0} \xi_j n_j \phi \exp\left(-\frac{\xi_k \xi_k}{2RT_0}\right) d\xi, \end{aligned} \tag{4}$$

where  $\alpha$  is the accommodation coefficient and  $n_i$  is the outward unit normal to the boundary. Fukui and Kaneko

[11] showed that for the air flow in the HDI, a solution satisfying Eq. 3 and compatible with the boundary condition Eq. 4 can be expressed as

$$\phi = \frac{1}{p_0} \frac{dp}{dx_1} x_1 + \frac{\xi_1}{\sqrt{2RT_0}} \phi_1(x_2, \xi_2, \xi_i \xi_i), \tag{5}$$

with  $\phi_1$  determined by

$$\frac{\lambda}{\sqrt{2RT_0}} \xi_2 \frac{\partial \phi_1}{\partial x_2} = \frac{\sqrt{\pi}}{2} \left( -\phi_1 + 2 \frac{U}{\sqrt{2RT_0}} \right) - \frac{\lambda}{p_0} \frac{dp}{dx_1}, \tag{6}$$

and

$$\phi_1|_{\xi_2 > 0} = (1 - \alpha_{\text{disk}}) \phi_1|_{\xi_2 < 0} + 2\alpha_{\text{disk}} \frac{U}{\sqrt{2RT_0}}, \tag{7}$$

$$\phi_1|_{\xi_2 < 0} = (1 - \alpha_{\text{slider}}) \phi_1|_{\xi_2 > 0}, \tag{8}$$

where the  $x_1$  direction is parallel to the disk, the  $x_2$  direction is perpendicular to the disk,  $p$  is the local pressure,  $dp/dx_1$  is the local pressure gradient,  $l$  is the length of the slider, and  $U$  is the disk speed. From Eq. 5 and kinetic theory [10], it can be shown that the shear force on the slider or the disk is a linear combination of contributions from the Couette and Poiseuille flow components.

For plane Poiseuille flow driven by a pressure gradient  $dp/dx_1$  and existing between two plates separated by a distance  $h$ , the momentum conservation equation, which is one of the first three moments of Eq. 1 with respect to  $\xi_i$ , can be simplified to

$$-\frac{dp}{dx_1} + \frac{\partial \sigma_{12}}{\partial x_2} = 0. \tag{9}$$

where  $\sigma_{12}$  is one component of the stress tensor.

Integrating Eq. 9 from the lower plate to the upper plate and using the symmetry of plane Poiseuille flow with respect to the center line, we get

$$\sigma_{12}|_{\text{upper plate}} = -\sigma_{12}|_{\text{lower plate}} = \frac{h}{2} \frac{dp}{dx_1}. \tag{10}$$

For plane Couette flow existing between two plates separated by  $h$  and with the lower plate fixed and the upper one moving at speed  $U$ , Sherman’s interpolation formula can be used [12]. This formula is based on an interpolation scheme between two limits: continuum flow and free molecular flow, and it has been shown to be consistent with experiments. For plane Couette flow of a continuum fluid, the shear force on the lower plate is

$$F_{\text{con}} = \mu \frac{U}{h}, \tag{11}$$

while for plane Couette flow of a free molecular gas for which the gas is so rarefied that the collisions between any two molecules are negligible, the shear force on the lower plate is [13]

$$F_{fm} = \frac{1}{2} \rho U \sqrt{\frac{2kT}{\pi m}}. \tag{12}$$

where  $\mu$  is the dynamic viscosity,  $m$  is the mass of the air molecule, and  $k$  is the Boltzmann constant. Then according to Sherman’s formula, the shear force on the lower plate in plane Couette flow of an arbitrarily rarefied gas is

$$F_c = F_{fm} \left\{ 1 + \frac{F_{fm}}{F_{\text{con}}} \right\}^{-1} = \frac{1}{2} \rho U \sqrt{\frac{2kT}{\pi m}} \frac{\mu}{\mu + \sqrt{\frac{1}{2} \rho h^2 \frac{2kT}{\pi m}}}. \tag{13}$$

Thus, the shear forces on the slider and the disk are:

$$\tau_w|_{\text{disk}} = F_c - \frac{h}{2} \frac{dp}{dx_1}, \tag{14}$$

$$\tau_w|_{\text{slider}} = -F_c - \frac{h}{2} \frac{dp}{dx_1}. \tag{15}$$

Before we can use these two formulae to calculate the shear forces, we need to know the pressure field and the viscosity. The first one, i.e., the pressure field, can be obtained from the generalized Reynolds equation while the second one can be modeled using the VSS model for air molecules.

### 3 The Generalized Reynolds Equation and the Variable Soft Sphere Model

#### 3.1 The Generalized Reynolds Equation

The classical Reynolds equation, which is derived from continuum theory, does not apply to air flow in the entire HDI, and the Boltzmann equation or its equivalent is needed. Under the same assumptions as in the classical Reynolds equation, i.e., the thickness of the air gap in the HDI is much less than the length and the width of the slider, and the air flow in the direction perpendicular to the disk is negligible, Fukui and Kaneko [11] started with the linearized Boltzmann equation, Eq. 3, and derived a generalized Reynolds equation for a steady flow in the HDI:

$$\left(\frac{b}{l}\right)^2 \frac{\partial}{\partial X_1} \left( Q_p P H^3 \frac{\partial P}{\partial X_1} \right) + \frac{\partial}{\partial X_2} \left( Q_p P H^3 \frac{\partial P}{\partial X_2} \right) = A_b \frac{\partial P H}{\partial X_1}, \tag{16}$$

where  $b$  is the width of the slider,  $l$  is the length of the slider,  $X_1 = x_1/l$ ,  $X_2 = x_2/b$ ,  $P = p/p_0$  is the nondimensional pressure,  $p$  is the air pressure,  $p_0$  is the ambient pressure,  $H = h/h_0$  is the nondimensional air gap thickness,  $h$  is the air gap thickness,  $h_0$  is the minimum air gap thickness,  $Q_p$  is the

nondimensional mass flow rate of the Poiseuille flow component,  $\Lambda_b = 6\mu Ub^2/(p_a h_0^2 l)$  is the bearing number,  $\mu$  is the air viscosity at the ambient state, and  $U$  is the disk speed.

The solution of Eq. 16 relies on two parameters: the bearing number  $\Lambda_b$  and the nondimensional mass flow rate  $Q_p$ . The bearing number depends on the air viscosity while the mass flow rate  $Q_p = Q_p(D, \alpha)$  is a function of the accommodation coefficient  $\alpha$  and the inverse Knudsen number  $D = \sqrt{\pi}h/(2\lambda)$  where  $\lambda$  is the mean free path. Since both  $\lambda$  and  $\mu$  are functions of temperature, the change in temperature affects the solution of the generalized Reynolds equation as well.

### 3.2 The Variable Soft Sphere Model

To investigate the dependence of the slider’s flying performance on the temperature, we need the formulae for the mean free path and the air viscosity as functions of temperature. These two formulae depend on the models used for the air molecules. The simplest one is the HS model, which regards the air molecules as rigid spheres with interaction between each other happening only at collision. One of the important quantities for collision is the angle  $\chi$  [1], as shown in Fig. 2.

For the HS model,  $\chi = 2\cos^{-1}(b/(2d))$  where  $d$  is the radius of air molecules and  $b$  is the projected distance. However, some macroscopic quantities calculated via the HS model, such as viscosity, can at most qualitatively agree with experimental results. The VSS model [14, 15] serves to improve the deficiency in the HS model while

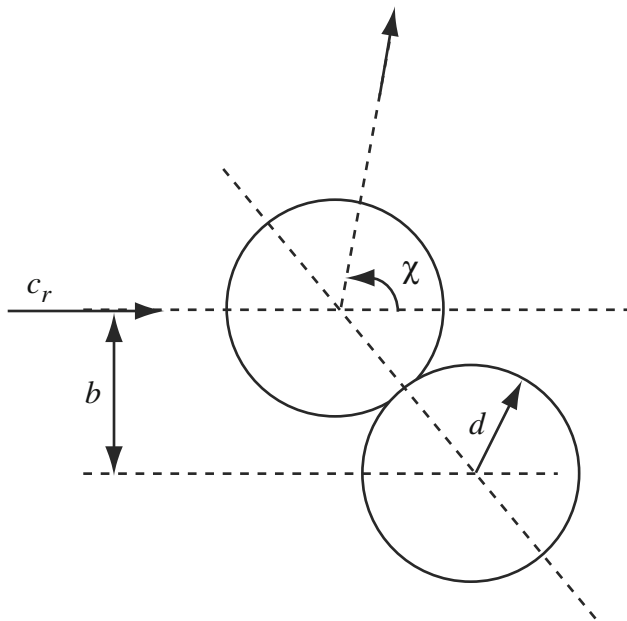


**Fig. 2** Collision between two air molecules with relative speed  $c_r$ . Here  $b$  is the projected distance,  $\chi$  is the angle after collision, and  $d$  is the radius of air molecules

keeping its simplicity. It is an empirical model with an empirical relation for  $d$  and  $\chi$  with parameters determined by fitting the experimental results. In the VSS model,  $d = d_{ref}(c_{r,ref}/c_r)^v$  and  $\chi = 2\cos^{-1}[(b/(2d))^{1/\eta}]$  where  $c_r$  is the pre-collision relative speed between two pre-collision molecules,  $v$  and  $\eta$  are two parameters used to fit experimental results, and the quantities with a subscript ref correspond to their values at a reference state. It can be shown that the mean free path for VSS molecules is [1]

$$\lambda = \frac{kT_{ref}}{\sqrt{2}\pi d_{ref}^2 4p} \left(\frac{T}{T_{ref}}\right)^{\omega+0.5}, \tag{17}$$

while the viscosity is

$$\begin{aligned} \mu &= \frac{5(\alpha + 1)(\alpha + 2)\sqrt{\pi mk}(4k/m)^v T^{v+0.5}}{16\alpha\Gamma(4 - v)\sigma_{ref}c_{r,ref}^{2v}} \\ &= \mu_{ref} \left(\frac{T}{T_{ref}}\right)^\omega \end{aligned} \tag{18}$$

where  $k$  is the Boltzmann constant,  $\omega = v + 1/2$ ,  $p$  is the air pressure,  $T$  is the temperature,  $\sigma$  is the collision cross section, and the quantities with a subscript ref correspond to their values at a reference state.

### 4 Results and Discussion

Equations 16–18 involve several reference quantities. Here we choose the following reference values [1, 16]:

$$\begin{aligned} T_{ref} &= 0^\circ\text{C}, & \mu_{ref} &= 1.81 \times 10^{-5} \text{Ns/m}^2, \\ d_{ref} &= 2.06 \times 10^{-10} \text{m} \\ m &= 5.6 \times 10^{-26} \text{kg}, & p_0 &= 1.013 \times 10^5 \text{N/m}^2 \end{aligned}$$

The finite volume method (FVM) [17] is used to solve the modified generalized Reynolds equation, Eq. 16, and it gives the pressure field in the HDI. The shear forces on the slider and the disk are then calculated with Eqs. 14 and 15. Two designs of the ABS, which is the surface of the slider facing the disk, are considered, and they are shown in Fig. 3. These two sliders are both Femto sliders (with length  $l = 0.85$  mm and width  $b = 0.7$  mm).

Figure 4 shows the change of the slider’s flying height at the read–write element with temperature for the two ABS designs. When flying over the inner track, slider A has a flying height of 7.47 nm at 25°C, and it decreases to 6.02 nm when the temperature increases to 95°C. When flying over the other two tracks, slider A has a higher flying height and the increase in temperature leads to a smaller change in the slider’s flying height. Similar trends occur for slider B. When slider B flies over the inner track, its flying height at the read–write element decreases from 5.59 to 4.08 nm when the temperature increases from 25 to 100°C.

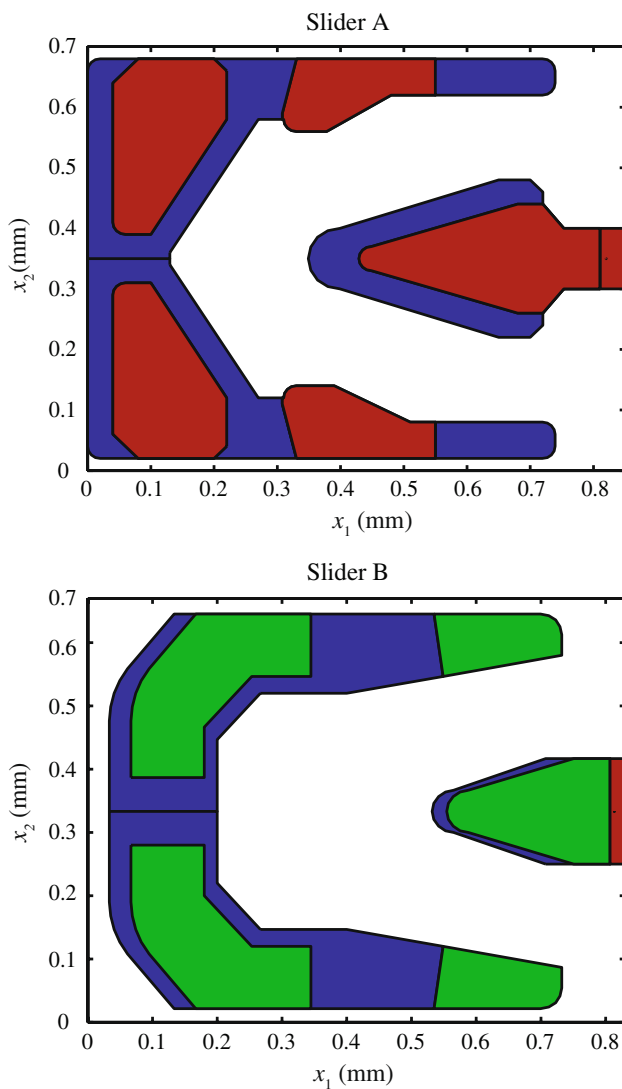


**Fig. 3** Air bearing surface of slider A and slider B. Both sliders are Femto sliders (with length  $l = 0.85$  mm and width  $b = 0.7$  mm). Different colors correspond to difference etching depths

Compared to slider A, slider B has a lower flying height, and the temperature increase has more effect on slider B. When both sliders fly at a height  $< 10$  nm, the temperature change induces a non-negligible change in the slider's flying height, and the lower the slider's flying height, the more the flying height decreases with the temperature.

As shown in Eq. 16, the slider's flying attitude is mainly determined by two parameters: the mean free path,  $\lambda$ , which appears in the calculation of mass flow rate of the Poiseuille flow component  $Q_p$ , and the air viscosity at the ambient state,  $\mu$ , which appears in the definition of the bearing number  $\Lambda_b$ . These two parameters increase with temperature, and they result in different changes in the slider's flying height: an increase in  $\lambda$  decreases the slider's flying height while an increase in  $\mu$  increases the slider's flying height [6]. The final trend of the change of the flying

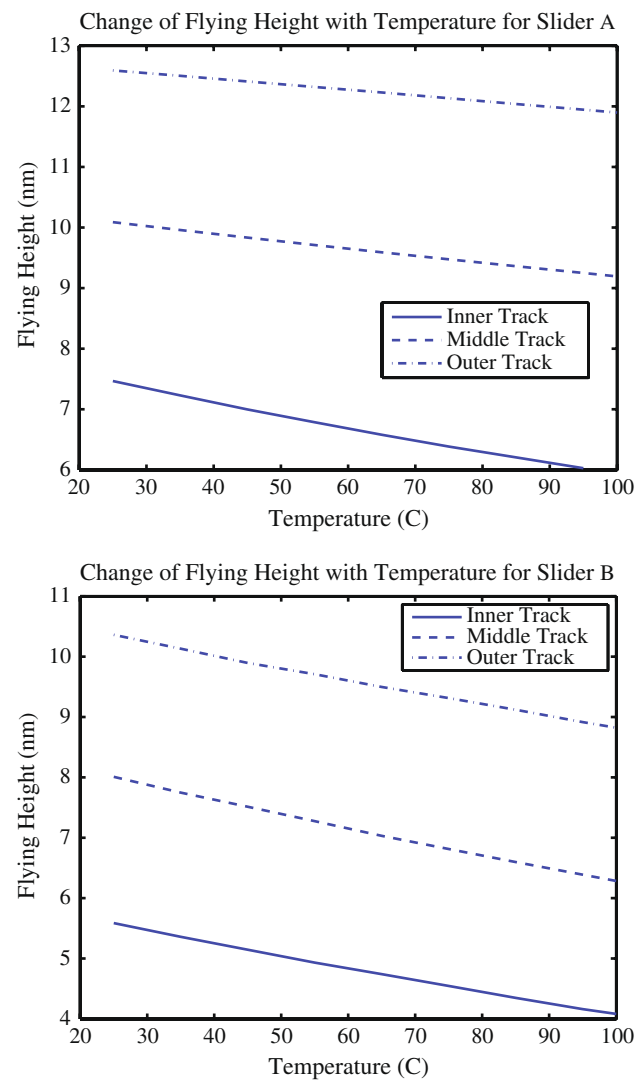


**Fig. 4** Change of the slider's flying height with temperature for the slider flying at the inner track, middle track, or the outer track

attitude with temperature is a net result of these two effects. For the two ABS designs studied in this paper, the slider's flying height decreases with temperature as shown in Fig. 4. The changes of the other two quantities of the slider's flying attitude, i.e., the slider's pitch and roll angles, are shown in Figs. 5 and 6. Since the pitch angle depends on a balance of the moments of the pressures on the front and rear parts of the sliders' surface, the decrease in the slider's flying height with temperature leads to different changes of the pressures on the front and the rear parts of the ABS, which results in the final increase of the sliders' pitch angle with temperature, as shown in Fig. 5. As for the roll angle, it is determined by a balance of the moments of the pressures on the left and right sides of the slider's surface. Since the ABSs of the two sliders are symmetric with respect to the centerline, the changes of the pressure with temperature are also symmetric about the centerline

and thus do not lead to noticeable changes of the roll angle. Although, for both slider A and slider B, the slider’s flying height decreases with temperature it is not guaranteed that this trend holds for all sliders, and opposite trends might exist for some other sliders. When comparing the results of slider A and slider B, we find that the effect of the temperature on the slider’s flying attitude also depends on the ABS designs. Thus, it might be possible to design a specific ABS pattern to reduce the dependence of the slider’s flying height on the temperature.

The shear forces on the slider and the disk are linear combinations of contributions of the Couette and Poiseuille flow components. Since the present problem has a large bearing number which is an indication of the importance of the Couette flow component compared to the Poiseuille flow component, the Couette flow component dominates the air flow. Thus only the shear forces due to the Couette flow component are presented in Figs. 7 and 8. For most regions on the ABS, the effect of temperature increase on

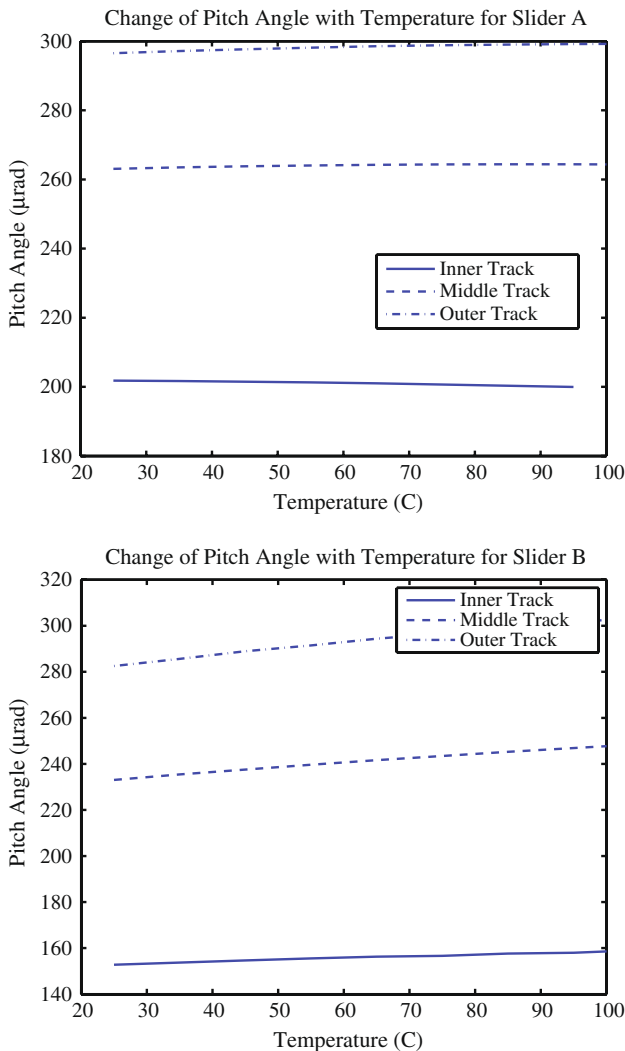


Fig. 5 Change of pitch angle with the temperature

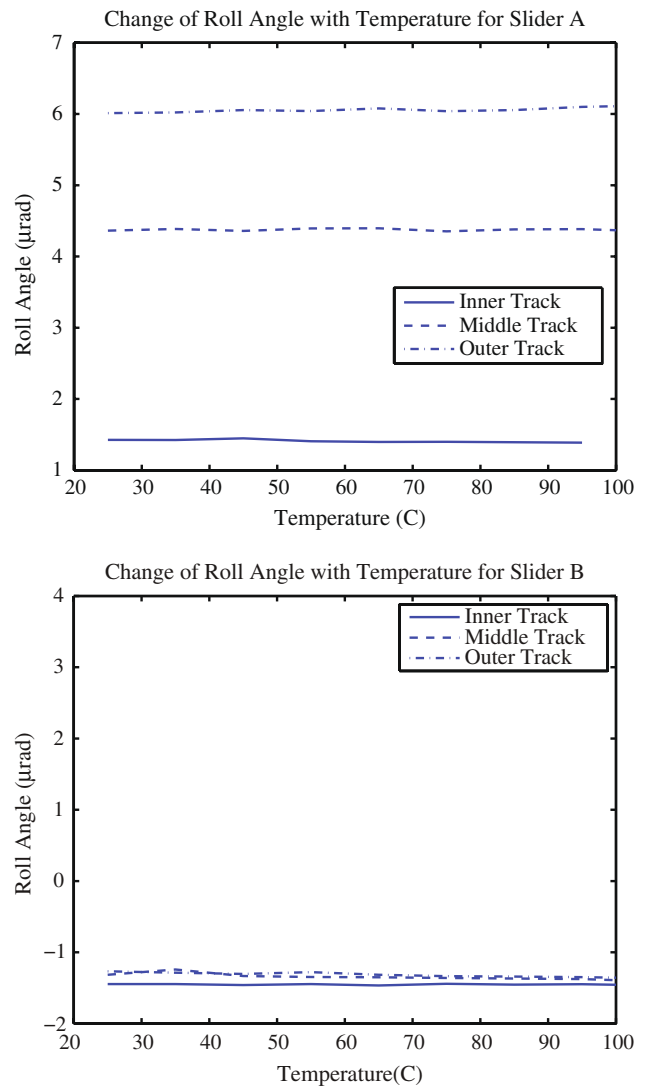
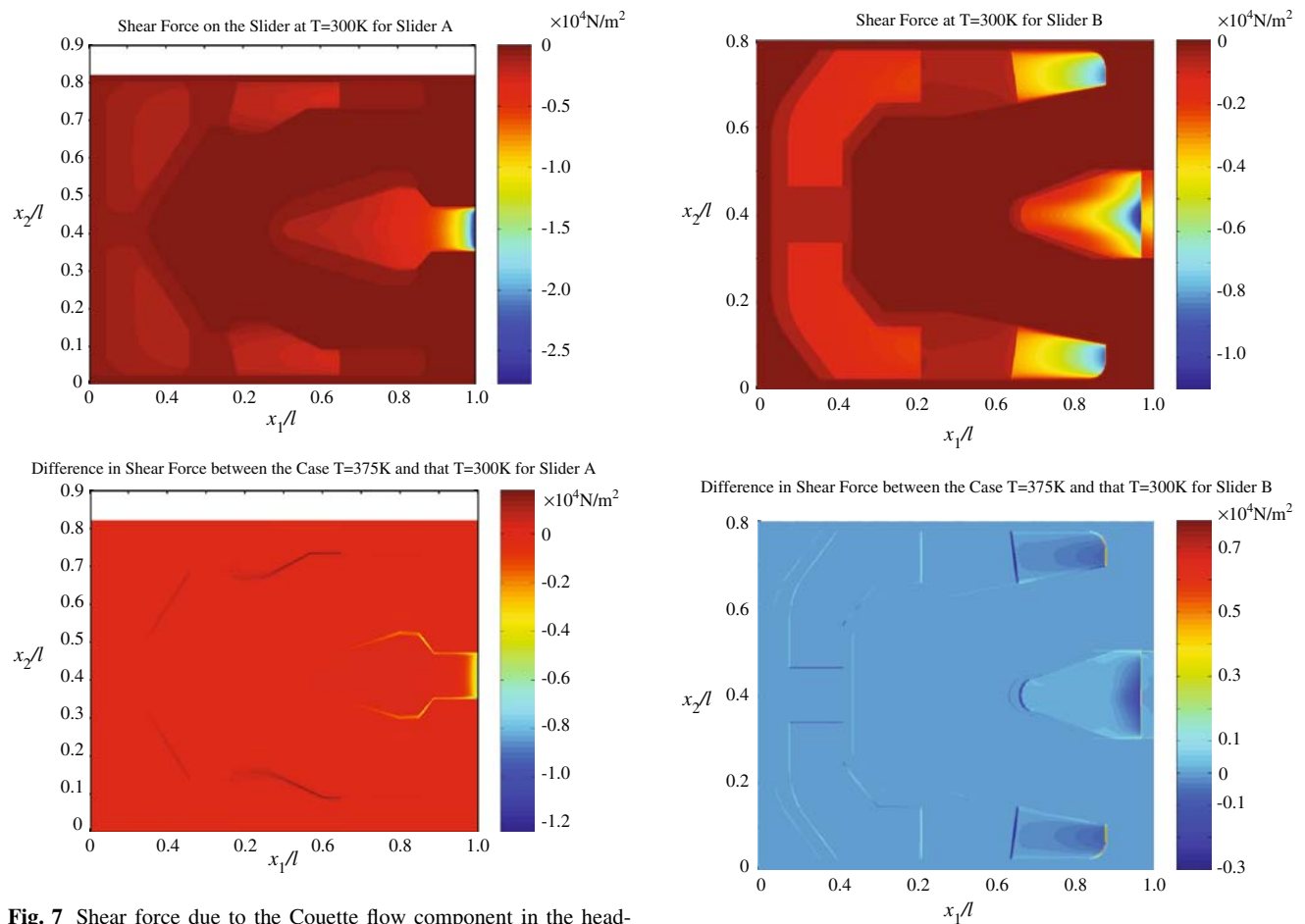


Fig. 6 Change of roll angle with the temperature

the shear force is negligible. The noticeable effect of the temperature increase on the shear force appears at the region near the read–write element, which is a combined effect of the decrease in the slider’s flying height and the increase in the slider’s pitch angle induced by the temperature increase. Since the slider’s flying height and its stability at the read–write element determine the HDDs’ capacity, changes of the shear force beneath the read–write element could result in changes in the deformation and instability of the lubricant, which may increase the possibility of the slider’s contact onto the disk and affect the reliability of the HDDs.

### 5 Summary and Conclusion

An approach to studying the effect of temperature change on a HDD slider’s flying attitude and the shear forces on



**Fig. 7** Shear force due to the Couette flow component in the head-disk interface for slider A. **a** The shear force at  $T = 25^\circ\text{C}$ . **b** The difference of the shear force at  $T = 25^\circ\text{C}$  from that at  $T = 100^\circ\text{C}$

the slider and the disk is presented in this paper. Based on the linearized Boltzmann equation and a similarity solution proposed by Fukui and Kaneko, we show that the shear forces are linear combinations of the contributions from the Couette and Poiseuille flow components. The former contribution is calculated through Sherman's formula, which interpolates the results for continuum flow and free molecular flow and generates a general formula applicable for an arbitrarily rarefied gas. The latter contribution is calculated through a formula derived from the conservation equations. These two formulae depend on the pressure gradient and the mean free path. The generalized Reynolds equation, proposed by Fukui and Kaneko and used to solve for the air flow field in the head-disk interface, is then modified to include the temperature effect on the mean free path and the air viscosity. These modifications are based on the variable soft sphere model, which is an empirical model that gives results agreeing well with experiments. The modified generalized Reynolds equation is solved using a FVM, and the shear forces are calculated afterwards. Numerical results are obtained for two slider designs, and the results show that the temperature change induces non-

**Fig. 8** Shear force due to the Couette flow component in the head-disk interface for slider B. **a** The shear force at  $T = 25^\circ\text{C}$ . **b** The difference of the shear force at  $T = 25^\circ\text{C}$  from that at  $T = 100^\circ\text{C}$ . Note that the zero value in this figure corresponds to a different color from that in Fig. 7

negligible changes in the slider's flying height as well as the shear force. Since these non-negligible changes are dependent on the ABS designs, it may be possible to design some specific ABS patterns to reduce the dependence of the shear force and the slider's flying height on the temperature.

**Acknowledgment** The authors thank Computer Mechanics Laboratory, Department of Mechanical Engineering at University of California at Berkeley for supporting this research.

**Open Access** This article is distributed under the terms of the Creative Commons Attribution Noncommercial License which permits any noncommercial use, distribution, and reproduction in any medium, provided the original author(s) and source are credited.

## References

- Bird, G.A.: Molecular Gas Dynamics and the Direct Simulation of Gas Flows. Oxford University Press, New York (1994)

2. Wallace, R.L.: The reproduction of magnetically recorded signals. *Bell Syst. Tech. J.* **30**, 1145–1173 (1951)
3. Marchon, B., Dai, Q., Nayak, V., Pit, R.: The physics of disk lubricant in the continuum picture. *IEEE Trans. Magn.* **41**, 616–620 (2005)
4. Kubotera, H., Bogy, D. B.: Effect of various physical factors on thin lubricant film migration on the flying head slider at the head-disk interface of hard disk drives. *J. Appl. Phys.* **102**, 054309 (2007)
5. Ma, Y., Liu, B.: Lubricant transfer from disk to slider in hard disk drives. *Appl. Phys. Lett.* **90**, 143516 (2007)
6. Cha, E., Chiang, C., Enguero, J., Lee, J.J.K.: Effect of temperature and attitude on flying height. *IEEE Trans. Magn.* **32**, 3729–3731 (1996)
7. Zhang, S., Strom, B., Lee, S.C., Tyndall, G.: Simulating the air bearing pressure and flying height in a humid environment. *ASME J. Tribol.* **130**, 011008 (2008)
8. Schaaf, S., Chambré, P.: *Flow of Rarefied Gas*. Princeton University Press, Princeton (1961)
9. Bhatnagar, H., Gross, E., Krook, M.: A model for collision processes in gases. I. Small amplitude processes in charged and neutral one-component systems. *Phys. Rev.* **94**, 511–525 (1954)
10. Sone, Y.: *Molecular Gas Dynamics: Theory, Techniques, and Applications*. Birkahuser, Boston (2006)
11. Fukui, S., Kaneko, R.: Analysis of ultra-thin gas film lubrication based on linearized Boltzmann equation: first report—derivation of a generalized lubrication equation including thermal creep flow. *ASME J. Tribol.* **110**, 253–261 (1988)
12. Sherman, F.S.: A survey of experimental results and methods for the transition regime of rarefied gas dynamics. In: Laurman, J.A. (ed.), *Rarefied Gas Dynamics*, pp. 228–260. Academic Press, New York (1963)
13. Vincenti, W.G., Kruger Jr., C.H.: *Introduction to Physical Gas Dynamics*. Wiley, New York (1965)
14. Koura, K., Matsumoto, H.: Variable soft sphere molecular model for inverse-power-law or Lennard-Jones potential. *Phys. Fluids A*. **3**, 2459–2465 (1991)
15. Koura, K., Matsumoto, H.: Variable soft sphere molecular model for air species. *Phys. Fluids A*. **4**, 1083–1085 (1992)
16. Lide, D. R.: *CRC Handbook of Chemistry and Physics*. CRC Press, Boca Raton, FL (2008)
17. Lu, S.: Numerical simulation of slider air bearings. Ph.D. thesis, Department of Mechanical Engineering, University of California, Berkeley, CA (1997)